

On the evolution of shape in N -body simulations

Ch. Theis¹, R. Spurzem²

¹ Inst. für Theoretische Physik und Astrophysik, Univ. Kiel, Olshausenstraße 40, D-24098 Kiel, Germany

² Astronomisches Rechen-Institut, Mönchhofstr. 12–14, 69120 Heidelberg, Germany

Received; accepted

Abstract. A database on shape evolution of direct N -body models formed out of cold, dissipationless collapse is generated using GRAPE and HARP special purpose computers. Such models are important to understand the formation of elliptical galaxies. Three dynamically distinct phases of shape evolution were found, first a fast dynamical collapse which gives rise to the radial orbit instability (ROI) and generates at its end the maximal triaxiality of the system. Subsequently, two phases of violent and two-body shape relaxation occur, which drive the system first towards axisymmetry, finally to spherical symmetry (the final state, however, is still much more concentrated than the initial model). In a sequence of models the influence of numerical and physical parameters, like particle number, softening, initial virial ratio, timestep choice, different N -body codes, are examined. We find that an improper combination of softening and particle number can produce erroneous results. Selected models were evolved on the secular timescale until they became spherically symmetric again. The secular shape relaxation time scale is shown to agree very well with the two-body relaxation time, if softening is properly taken into account for the latter. Finally, we argue, that the intermediate phase of violent shape relaxation after collapse is induced by strong core oscillations in the centre, which cause potential fluctuations, dampening out the triaxiality.

Key words: Numerical methods – Galaxies: kinematics and dynamics – Galaxies: evolution

1. Introduction

Formation scenarios of elliptical galaxies are either based on merging of galaxies or on violently collapsing stellar systems (or on combinations of both). Especially the field ellipticals most likely pass through a phase of cold dissipationless collapse. It only occurs if the primordial gas cloud forming a galaxy has a very efficient phase of star formation at the beginning by which practically all the gas is transformed into stars. Thereafter the system is not supported against further collapse until a dynamical equilibrium is reached. The structure of the final state is restricted by the time-independent tensor-virial theorem (see Binney & Tremaine 1987), which includes the possibility of anisotropy-supported triaxial configurations.

Send offprint requests to: Ch. Theis

Merritt & Aguilar (1985) and Min & Choi (1989) have shown by N -body simulations that the initially spherical system does not remain spherical during collapse. If approximately $2T/|U| < 0.1$, where T and U are the kinetic and potential energy of the initial state, the system is unstable against the formation of a nearly prolate shape. Aguilar & Merritt (1990) performed an exhaustive study of the final shape of the prolate configuration as a function of initial parameters as kinetic energy and initial triaxiality. Cannizzo & Hollister (1992) varied in a similar parameter study the initial density profile and the softening parameter (three values).

This instability, commonly known as “radial orbit instability” (henceforth ROI) was long believed to be connected with some initial amount of anisotropy in the velocity dispersions of the system, which either stems from the initial conditions or develops during collapse. However, Udry (1993) showed that even a very small initial anisotropy suffices to develop ROI, and more recently Hozumi, Fujiwara & Kan-ya (1996) pointed out that the onset of ROI happens during the collapse of a uniform sphere while it remains completely isotropic. So, although it is usually stated that the onset of ROI can be understood as a type of Jeans instability perpendicular to the radial movement of collapse, a complete understanding of its mechanism is still lacking. It is interesting to note, however, that some remarks made by Bettwieser & Spurzem (1986) and Hensler et al. (1995) can be applied here. They showed that homogeneous systems in self-similar collapse remain exactly isotropic, whereas in other cases anisotropy develops proportional to the gradient of u/r , where u is the radial bulk mass streaming velocity.

ROI is related to the concept of global instability of stellar systems, although details of this relation are still unclear. The global instability of a spherical system of purely radially moving stars had been proven by Antonov (1961) and Polyachenko & Shukhman (1981) analytically. Most other analytic or semi-analytic stability criteria rely on an energy principle, but can be applied only to systems where the distribution function is a function of energy alone, i.e. isotropic systems (Antonov 1961, 1962, Lynden-Bell 1964, Ipser & Thorne 1968, Kulsrud & Mark 1970). For most anisotropic and more realistic cases, however, no rigorous proof of sufficient or necessary criteria for stability is known, and one has to rely on numerical simulations, as in the papers cited in the previous paragraphs.

Lynden-Bell (1967) derived by using principles of statistical mechanics a most probable distribution function as the

end-state of cold, dissipationless collapse, the Lynden-Bell distribution. The assumed nature of the process led to the notion of violent relaxation. However, already very early N -body simulations (Cuperman, Goldstein & Lecar 1969) were not able to show that such a distribution occurs. Burkert (1990) tried to relax the problem by assuming that the relaxation is incomplete, i.e. not all elements of phase space are accessible with equal probability, but the concept of violent relaxation thereby became not so attractive anymore. There was a remarkable series of papers (Wiechen, Ziegler & Schindler 1988, Ziegler & Wiechen 1989, 1990), who derived the final state as a function of the initial state by an energy principle. However, it has not yet been practically applied, as far as the authors of this paper are aware of.

Hence direct N -body simulations still are the appropriate tool to examine cold dissipationless collapse. In recent years significant advances in hardware and software for direct N -body simulations have been made. On one hand TREE codes (Barnes & Hut 1986) have been ported to parallel computers and coupled with particle based hydrodynamic simulations (TREE-SPH, Davé et al. 1997). On the other hand completely different approaches like grid-based schemes (Udry 1993) or the self-consistent-field method (SCF) by Hernquist & Ostriker (1992) have been successfully used for stellardynamical applications (e.g. in the case of cold collapse Hozumi & Hernquist 1995). Although e.g. the latter appear to be ideally suited for collisionless systems, because they do not use particle-particle forces to integrate the orbits, they suffer from their inflexibility in adaptation to different applications and resolutions (basically for every new application an appropriate set of basis functions to evaluate the potential has to be searched, and the attempt to increase small-scale resolution, e.g. in angular direction, increases the CPU time nearly as inhibitive as for direct N -body simulations, since CPU time goes roughly with n^2 , where n is the number of terms in the series evaluation for tangential resolution, much like a force calculation scales with N^2 where N is the total particle number).

Thus, even for collisionless systems and applications with correspondingly very large particle numbers, direct or at least TREE-like N -body simulations will remain very useful and important in the foreseeable future because of their inherent Lagrangian nature, yielding high resolution at high density regions automatically. Moreover, we think it is not fully clear what is the physically correct case for a collapsing protogalaxy. On one hand, the collapse might occur in a system consisting of protogalactic clouds of masses as large as say $10^6 M_\odot$ (cf. e.g. Theis & Hensler 1993, 1995); in such case a collisionless approach like in the case of SCF codes does not represent the physical situation. On the other hand, even considering a collapsing system made out of billions of stars only, some relaxation effects (not necessarily just two-body relaxation) can occur on timescales much shorter than the standard two-body relaxation time. It is not clear and deserves further comparison between the different approaches whether a mean field based or a direct N -body method (using large N and very small softening) represent a more accurate representation of the real physical system under study.

For the direct N -body simulations special purpose computers have been very successfully built (Sugimoto et al. 1990, Makino et al. 1997) and applied (Makino 1996, Makino & Ebisuzaki 1996, Makino 1997). There are different versions of such machines e.g. for high precision (collisional stellar dynam-

ics, HARP, GRAPE-4) and low precision (collisionless systems, GRAPE-3, GRAPE-5). We have used the GRAPE 3Af and HARP-2 special purpose computers in Kiel and Heidelberg to produce a data base on the influence of the softening length and the particle number on the evolution of the shape (axis ratios) of stellar systems during cold collapse and ROI. Due to the use of GRAPE 3Af (4.8 Gflop peak performance) our data could cover simultaneously small softening and large particle number N . The use of HARP-2 enabled us to provide data without any softening for comparison. Small softening should increase two-body relaxation, whereas large N decreases it (compared to the dynamical timescale). In a real galactic system ε should be vanishing for all practical purposes, since the radii of the stars are extremely small relative to the mean interparticle distance. On the other hand, the particle number is so large as well (e.g. 10^{11}) that the standard two-body relaxation time is large compared to the age of the universe. Since a direct model with $N = 10^{11}$ and a vanishing softening length ε is impossible now and in the near future by a wide margin, generally a system with very different N and ε is used, very often just in the vague hope that ε is large enough to render all two-body relaxation effects unimportant during the simulation and to use N as large as possible with the present computer generation (compare Theis 1998). As for the evolution of the shape of triaxial galaxies, emerging after cold collapse of an initially extended gas-free stellar system, we will show that relaxation effects still play an unwanted role in the simulations. As a result we conclude that great care should be taken in interpreting results of such N -body simulations as models of real galaxies.

2. Numerical Results

2.1. The reference model

In our reference model (model A1) we started with $N = 32768$ particles of total mass $M = 1$. The particles were distributed according to a Plummer density profile

$$\rho(r) = \rho_0 \cdot (1 + (r/r_0)^2)^{-5/2}. \quad (1)$$

The units are normalized to a gravitational constant $G = 1$, a unit mass and a total potential energy $U = -1/2$. For a virialized system the latter choice guarantees a normalization to the standard N -body units. However, here we start with a cold system (i.e. the total energy $E \approx U$) resulting in a crossing time $t_{\text{cr}} \equiv (GM^{5/2})/\sqrt{2|E|}^3 \approx 1.03$, for a virial ratio $\eta_{\text{vir}} \equiv 2T/|U| = 0.04$. (T is the total kinetic energy.) The mass distribution corresponds for a Plummer model to an initial scale radius $r_0 = 3\pi/16 \approx 0.589$ giving a free-fall time at the scale radius of $t_{\text{ff}}(r_0) \equiv \sqrt{3\pi/(32G\bar{\rho}(r_0))} \approx 0.84$. $\bar{\rho}(r)$ is the average mass density inside a sphere of radius r . The initial velocities were chosen according to an isotropic Gaussian distribution with a velocity dispersion that results in an initial virial coefficient $\eta_{\text{vir}} = 0.04$. Thus, the collapsing system is prepared to form a triaxial system via a ROI (Aguilar & Merritt 1990).

The gravitational softening length was set to $\varepsilon = 0.01$ which is a factor of two smaller than the average interparticle distance $r_n = r_0/\sqrt[3]{N}$ at the center and a factor of 1000 larger than the average 90° deflection impact parameter $p_0 = r_0/(2N) \approx 9 \cdot 10^{-6}$. In opposition to select ε large enough

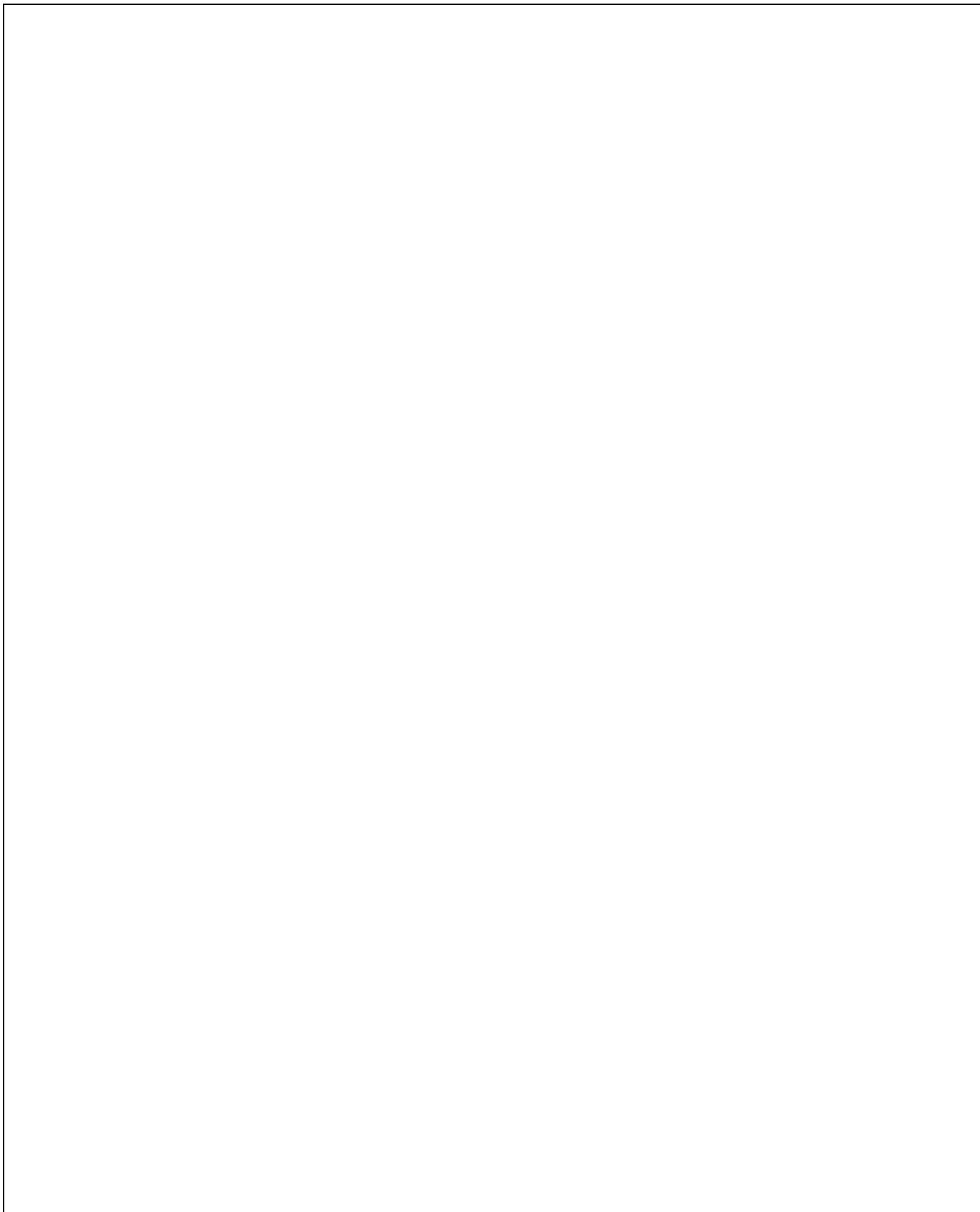


Fig. 1. Projection of the particles on the (arbitrary) x - y -plane at different times (from upper left to lower right: $t = 0, 1.5, 2.5, 5.0, 20.0, 200.0$). The simulation was performed with $N = 32768$ particles and a softening length $\varepsilon = 0.01$ (model A1).

to have little undesired two-body relaxation we here want to examine the different shape evolution of systems with small and large softening after and during the so-called “cold collapse”. It is our aim by this method to study the influence of varying degrees of two-body relaxation on the results. The time integration in the simulations was performed with a leap-frog scheme using a fixed timestep of $\Delta t = 0.0015$ which is less than 0.3 per cent of the central free-fall time. This small timestep is the price for an acceptable energy error in the numerical simulation of the collapse of an initially cold configuration when a small gravitational softening is applied. The energy conservation is in all simulations better than 0.2 per cent, mostly better than 0.05 per cent. (Typically the energy error is at maximum in the collapse phase, whereas later on the energy fluctuations are an order of magnitude smaller than the largest deviation.) The potential was evaluated by a GRAPE 3Af special purpose computer which applies the standard Plummer softening, i.e. the acceleration \mathbf{a}_{ij} of particle i by particle j is calculated by

$$\mathbf{a}_{ij} = \frac{Gm_j}{(r_{ij}^2 + \varepsilon^2)^{3/2}} \mathbf{r}_{ij}, \quad (2)$$

The temporal evolution of the system starts with a strong collapse. After a typical collapse time $t_{\text{ff}}(r_0)$ of the system the central region begins to reexpand whereas the outer layers are still falling to the center because of their larger free-fall time. Three collapse times later the inner 75 per cent of the system reach an equilibrium state, i.e. the Lagrangian radii remain almost constant. The half-mass radius has decreased by a factor of 1.6 compared to the initial value and the inner Lagrangian radii are typically smaller by a factor 3–5. The relatively small decrease of the half-mass radius is a result of the change in the shape of the system: During the first collapse phase the system remains spherical, which is consistent with the results of Hozumi, Fujiwara & Kan-ya (1996). The shape however changes quickly afterwards, when the central region reexpands (Fig. 1). After $t = 1.79t_{\text{ff}}(r_0) = 1.5$ a central bar-like structure can be identified which becomes more and more dominant until $t = 2.5$. The shape is now almost fixed in the sense that it does not vary significantly on a crossing timescale. However, due to relaxation processes which are discussed below there is a secular evolution towards a more spherical mass distribution (Fig. 1). The dynamics of the central part can be followed by the evolution of the core parameters and the density centre. In Fig. 2a the density weighted core radius r_{core} defined in the same way as the density radius in Casertano & Hut (1985) decreases strongly during the collapse phase and reaches an equilibrium value of 0.04 at $t = 2.0$. The corresponding core mass drops from 0.17 for the initial Plummer model to a final core mass $M_{\text{core}} = 0.05$. Once the equilibrium state is reached, both values vary only by 10% during the whole simulated evolution (until $t = 200$) which demonstrates the remarkable constancy of the core properties. The motion of the density centre will be described later in Sect. 3.

The flattening of the mass distribution is calculated by transformation to the principal axes of the tensor of inertia relative to the density centre of the system using different numbers of particles which are sorted by their binding energy. For 50% of all bound particles one finds that the minor to major axis ratio c/a begins to decrease at $t = 0.8$ and reaches a minimum of 0.36 at $t = 3.0$ (Fig. 2b). Afterwards the axis ratio increases linearly to 0.52 at $t = 20$. The intermediate-to-major axis ratio b/a shows a similar behaviour as c/a : With

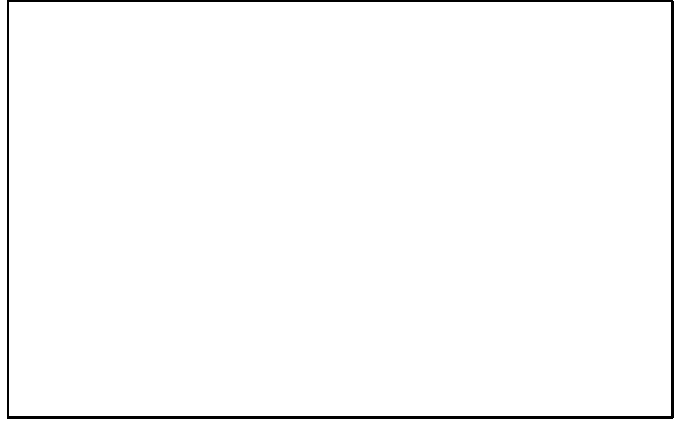


Fig. 2a. Temporal evolution of the core radius (solid) and the core mass (dashed) for model A1 ($N=32768$, $\varepsilon = 0.01$).

a short delay of $\Delta t = 0.2 b/a$ starts to decrease at $t = 1.0$ and reaches a minimum of 0.42 at $t = 3.0$. Later on, the ratio c/a is on average 0.1 less than b/a which indicates a slightly triaxial (but near to prolate) system characterized by a triaxiality parameter $\tau \equiv (b - c)/(a - c)$ in the range of 0.15 to 0.25. In the central region, i.e. the inner most 10 per cent, the decrease of the axis ratios begins at the same time as at the half mass radius, but they are typically larger by 0.1–0.15 (Fig. 2b). The flattening of the halo region, i.e. the 90 per cent most bound particles, is weak and strongly delayed according to the enhanced collapse time in the outer region. Additionally, the isotropic redistribution of particles gaining energy in the violent relaxation phase leads to a more spherical structure of the halo.

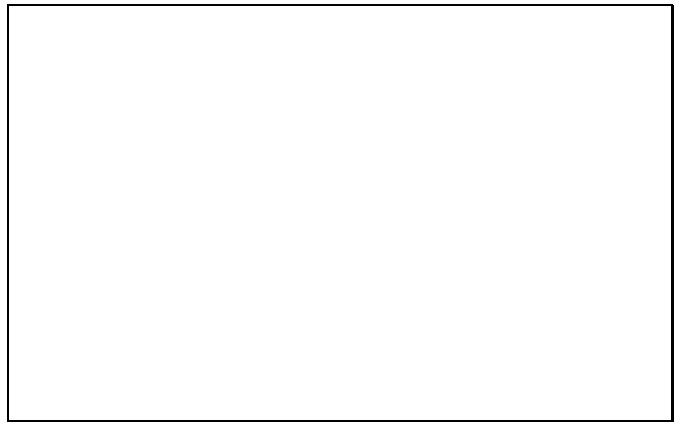


Fig. 2b. Temporal evolution of the minor-to-major axis ratio in the centre (10% most bounded particles, upper curves after collapse) and at the half-mass radius. The softening length was set to $\varepsilon = 0.01$ (dashed, model A1) and $\varepsilon = 0.1$ (solid, model B1) with $N = 32768$. Note here and in the following figures that the timescale of the first collapse of the central region is constant and is equal to $t_{\text{ff}}(r_0) \approx 0.84$ for all models.



Fig. 2c. Temporal evolution of the Lagrange radii for a model with $N=4096$, no softening (+, HARP) and a simulation with $\varepsilon = 0.01$ (solid, GRAPE, model D).

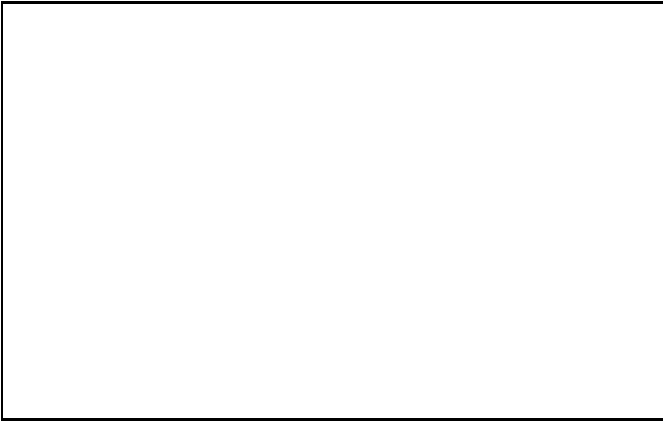


Fig. 2d. As Fig. 2c, but for $N=16384$ (GRAPE, model F).

2.2. A parameter study

In order to check the influence of the parameters used in N -body simulations we selected one reference model (A1) and then varied its parameters in a sequence of models. Physically we changed the gravitational softening length ε (models B1-3 and C), the total number N of the particles (models D, F), and ε and N simultaneously so as to keep the ratio of ε to the mean interparticle distance constant (model E). In order to study the influence of softening on the long-term evolution of the quasi-equilibrium configuration formed after ROI, two simulations with different softening, but identical configurations as model F at $t = 20$ were performed (models G, H). For the two models I and J the initial virial coefficient was changed from the reference value $\eta = 0.04$ to $\eta = 0.2$ in order to compare our models with the results of Aguilar & Merritt (1990). To test the intrinsic errors of our program we varied in models A2 and B2 the random number set used to initialize the particle configuration, and in model A3 and B3 a significantly larger (constant) time step was used (increased by a factor of 10 as compared to the reference model). For model A3 with the small softening length of 0.01 it led to intolerable errors of the energy "conservation" ($\sim 90\%$), so this model was discarded for the data evaluation (see also Sect. 2.2.4).

For all models with small initial virial coefficient the collapse of the core proceeded in one free-fall time; Figs. 2c,d depict the evolution of Lagrangian mass shells containing the indicated fraction of total mass for $N = 4096$ and $N = 16384$. For comparison data of a run using HARP-2 and a different N -body integrator (NBODY6++, Spurzem 1998) without any softening are given. The excellent agreement of both results tells us that for the reference model there are no more softening-dependent effects in the simulation during the collapse timescale up to the maximum particle number used in our HARP simulations (16384), hence the softened model is dynamically equivalent to the "real" discrete system. This however, has to be proven again when increasing N further.

Only after the maximum central density in the collapse is reached strong deviations of the shape of the system from spherical symmetry (generally triaxiality) occur (as can be seen by comparing Figs. 2b and 2c,d). According to Hozumi, Fujiwara & Kan-ya (1996) this could be ascribed to the ROI producing strongly anisotropic velocity dispersions, which then give rise to a non-spherical equilibrium system.

Tables 1-3 give an overview for all models presented here, first the model parameters (Table 1), and thereafter some typical values describing the flattening (small and intermediate axes relative to the major axis, and its time derivative) with the timescale t_{\min} defined as the time of minimum c/a (which is almost identical to the time of minimum b/a). Note that t_{\min} is larger than the collapse time of the core.

As a general conclusion from Tables 2 and 3 one could already deduce that small softening tends to increase the rate of change of c/a after the system has become flattened. At a first glance this could be interpreted as a stronger effect of two-body relaxation present in these systems. However, we will argue in the following that more caution is necessary in the interpretation of the data.

Table 1. Model parameters for the numerical simulations

model	N	ε	η_{vir}	Δt	comment
A1	32768	0.01	0.04	0.0015	reference model
A2	32768	0.01	0.04	0.0015	different random set
A3	32768	0.01	0.04	0.015	large energy error
B1	32768	0.1	0.04	0.0015	
B2	32768	0.1	0.04	0.0015	different random set
B3	32768	0.1	0.04	0.015	
C	32768	0.02	0.04	0.0015	
D	4096	0.01	0.04	0.0015	
E	4096	0.02	0.04	0.0015	
F	16384	0.01	0.04	0.0015	
G	16384	0.02	0.04	0.0015	
H	16384	0.1	0.04	0.0015	
I	32768	0.01	0.2	0.0015	
J	4096	0.01	0.2	0.0015	

2.2.1. The softening

For the investigation of the effect of softening we increased ε by a factor 10 to 0.1 which is a factor of 5 larger than the mean central interparticle distance (model B1). Fig. 2b shows that the deviation from sphericity for half of the particles is now delayed by a factor 2.5–3 compared to the reference model A1

Table 2. Flattening parameters of the 50% most bound particles

model	t_{\min}	$\frac{c}{a}_{\min}$	$\frac{b}{a}_{\min}$	$\frac{c}{a}_{\text{fin}}$	$\frac{b}{a}_{\text{fin}}$
A1	2.9	0.36	0.41	0.48	0.57
A2	3.9	0.36	0.41	0.52	0.65
B1	6.6	0.34	0.39	0.35	0.42
B2	7.1	0.37	0.39	0.38	0.42
B3	6.6	0.34	0.38	0.38	0.44
C	4.0	0.34	0.39	0.46	0.57
D	3.3	0.39	0.42	0.54	0.57
E	4.3	0.35	0.41	0.50	0.58
F	3.7	0.35	0.40	0.52	0.57

The models G and H are omitted because they start with the configuration of model F at $t = 20$. The dynamically hot models I,J are omitted since they do not flatten significantly. Model A3 is omitted because energy conservation is not sufficient. The final time corresponds here to $t = 20$.

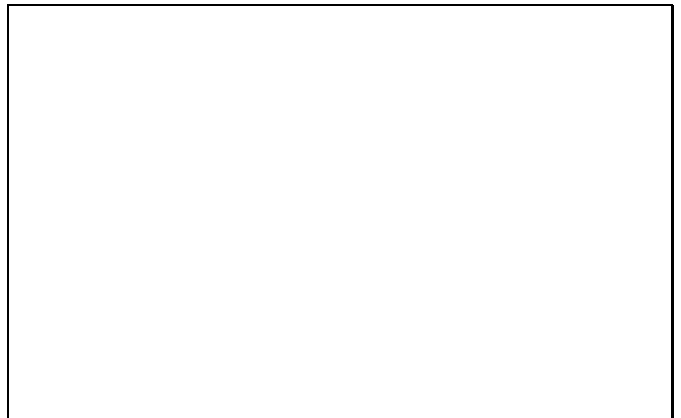
Table 3. Flattening parameters of the 10% most bound particles

model	t_{\min}	$\frac{c}{a}_{\min}$	$\frac{b}{a}_{\min}$	$\frac{c}{a}_{\text{fin}}$	$\frac{b}{a}_{\text{fin}}$
A1	2.9	0.53	0.55	0.62	0.64
A2	4.1	0.53	0.56	0.65	0.71
B1	6.8	0.78	0.80	0.77	0.80
B2	7.0	0.76	0.79	0.76	0.79
B3	6.5	0.78	0.80	0.77	0.78
C	4.0	0.54	0.56	0.60	0.63
D	2.1	0.67	0.72	0.81	0.87
E	4.3	0.66	0.70	0.67	0.71
F	2.8	0.60	0.61	0.71	0.77

Models G,H,I,J,A3 are omitted for the same reasons as in Table 2. The final time corresponds here to $t = 20$.

with a smaller softening. The minimum axis ratio c/a reaches 0.34 at $t = 6.65$ for the 50 per cent most bound particles which is almost the same minimum value as in model A1. Until the end of the simulation c/a increases only very slightly to 0.35.

Here we find two quite different effects of a variation of softening. First, the build-up of non-sphericity needs more time if softening is larger. This is valid for both the 10% and the 50% most bound particles. Second the difference between the shape of the 10% and the 50% most bound particles is smaller for small softening. Or, in other words, decreasing the softening makes the 10% most bound particles less spherical, but the 50% most bound particles more spherical. We interpret such results as follows: first the initial collapse proceeds to much deeper central potential in the case of small softening. So the effect of the ROI is stronger, which explains the difference in t_{\min} of the two cases. The term stronger here means that the timescale for the build-up of deviations from spherical symmetry is smaller, as well as a smaller numerical value of c/a for the 10% most bound particles.

**Fig. 3.** Temporal evolution of the minor-to-major axis ratio in the centre (10% most bounded particles) and at the half-mass radius. The number of particles has been set to $N = 32768$ (solid, model A1) and $N = 4096$ (dashed, model D) with a softening length $\varepsilon = 0.01$.**Fig. 4.** Temporal evolution of the minor-to-major axis ratio in the centre (10% most bounded particles) and at the half-mass radius. The number of particles has been set to $N = 32768$ (solid, model A1) and $N = 4096$ (dashed, model E) with a softening length $\varepsilon = 0.01$ (model A1) and $\varepsilon = 0.02$ (model E), respectively.

2.2.2. The number of particles

The effect of a variation of the particle number at constant softening is shown in Fig. 3. While until the time t_{\min} differences are very small, ROI proceeds to stronger perturbations of the spherical shape in the inner shells (10%) for larger N .

In the models D and E we decreased the total number of particles to $N = 4096$ and performed the calculation with two different softening lengths: $\varepsilon = 0.01$ (model D) and $\varepsilon = 0.02$ (model E). Until c/a reaches its minimum value at $t = 3.0$ the temporal evolution of the axis ratio inside the 50 per cent region are very similar to the reference model A1 with the same softening, but an increased particle number of $N = 32768$ (Fig. 3). We conclude that until t_{\min} the ROI measured at the half-mass radius does not depend strongly on the number of particles, but only on the depth of central potential reached. This supports that the onset of ROI is a collective effect.

In model E the softening length is a factor 2 larger than in model A1 and D. This means that the ratio of the softening length to the average particle distance is the same for the ref-

erence model A1 and model E. In the central region the larger softening induces a finally increased c/a of 0.7 (Fig. 4). As in the previous case larger N generally increases the strength of ROI in the inner parts of the system. However, small differences in the evolution of the 50% mass shell can be compensated by our variation of $\varepsilon \sim 1/\sqrt[3]{N}$. This suggests that gravitational scattering plays a role here. However, classical two-body relaxation by particle-particle interaction (e.g. Spitzer & Hart, 1971) is too slow to explain the observed compensation. Thus, the scattering of particles with the massive and much more concentrated core of the system as a whole might cause the relaxation here. This point will be discussed in Sect. 3 in more detail. We are grateful to T. Tsuchiya (pers. communication) to point this out to us as a possible mechanism.

2.2.3. The virial coefficient

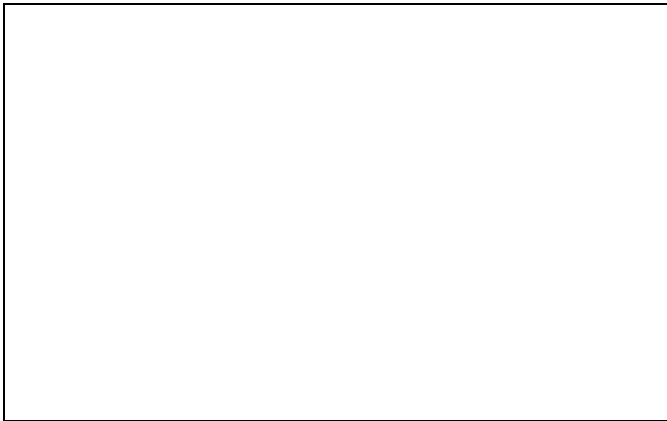


Fig. 5. Temporal evolution of the minor-to-major (c/a) and intermediate-to-major (b/a) axis ratio for the 50% most bounded particles. The initial virial coefficient has been set to $\eta_{\text{vir}} = 0.04$ (solid, model A1) and $\eta_{\text{vir}} = 0.2$ (dashed, model I). Both models were calculated with $N = 32768$ and $\varepsilon = 0.01$.

We studied the influence of the initial distribution in velocity space by starting with a dynamically “warm” configuration for the spatial configurations of the models A1 and D, i.e. a virial coefficient $\eta_{\text{vir}} = 0.2$ (models I ($N = 32768$) and J ($N = 4096$)). In agreement with Aguilar & Merritt (1990) and Boily et al. (1998) the memory to the initial conditions is preserved and the system remains almost spherical throughout the simulations when starting from spherical initial configurations (Fig. 5). Within statistical errors the models do not depend on the total number of particles.

2.2.4. Miscellaneous

In a set of models we investigated the influence of numerical effects introduced by the chosen timestep (models A3 and B3) and the random realization of the initial particle distribution (models A2 and B2). If the timestep is increased by an order of magnitude (model A3) the energy is only well conserved (better than 1.5 per cent) for a model with a large softening of $\varepsilon = 0.1$ (H), whereas the small softening of the reference model introduces a very large integration error at the moment of strongest compression. If we perform the simulation of model A1 with a doubled timestep, the results are almost identical to the reference model.

For several models we performed the simulations with other sets of initial configurations (e.g. models A2 and B2). Generally, the deviations of the axis ratios are less than 5 per cent, until dynamical equilibrium has been established, i.e. until $t \approx 5$. However, the relaxation timescale seems to vary slightly which gives an intrinsic error of c/a of 0.04 at the end of most of the simulations ($t = 20$). Thus, our results do not critically depend either on the chosen timestep or on the randomly chosen initial particle configuration.

2.3. The long-term experiments

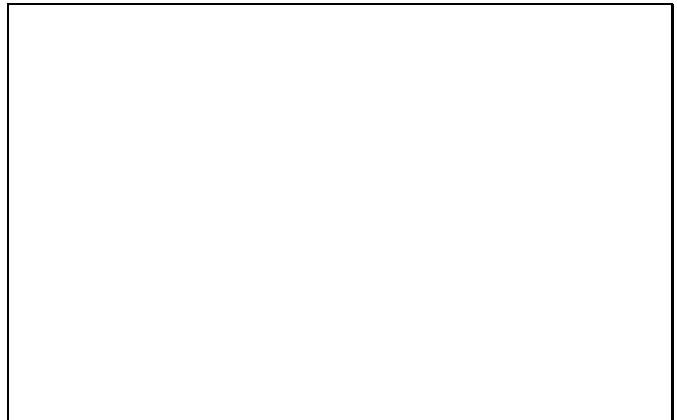


Fig. 6. Long-term evolution of the intermediate-to-major axis ratio (solid) and the minor-to-major axis ratio (dashed) at the half-mass radius for a simulation with $N = 16384$ particles. The softening length was set to $\varepsilon = 0.01$ (model F).

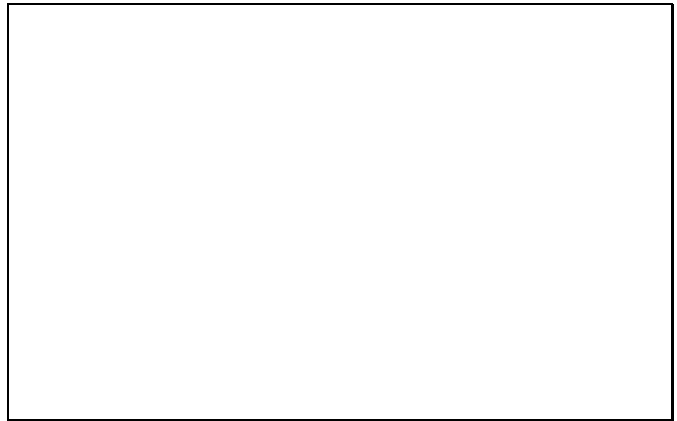


Fig. 7. Long-term evolution of the minor-to-major axis ratio at the half-mass radius for simulations with $N = 4096$ (solid, model D) and $N = 16384$ (dashed, model F) particles. The softening length was set to $\varepsilon = 0.01$. The straight lines correspond to a spherization of the system in one relaxation time (the latter is already corrected for softening).

In some cases we followed the evolution of the system for a much longer time, until it practically relaxed again to a spherically symmetric configuration (models A1, C, D, E, F, G and H). The evolution of shape shows three different phases (e.g.

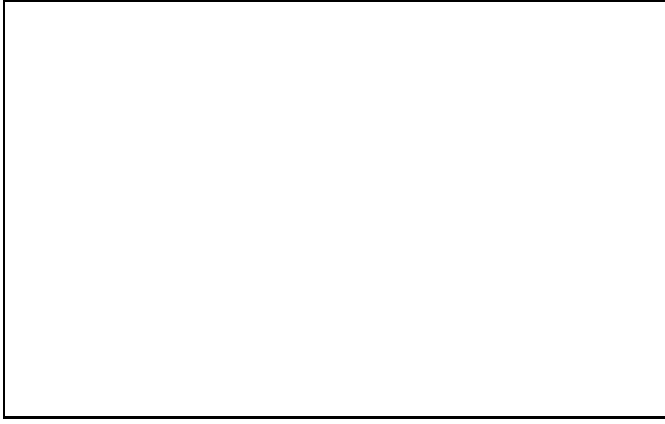


Fig. 8. Long-term evolution of the (logarithmic) deviation from sphericity at the half-mass radius for simulations with $N = 4096$ (solid, model D) and $N = 16384$ (dashed, model F) particles. The softening length was set to $\varepsilon = 0.01$.

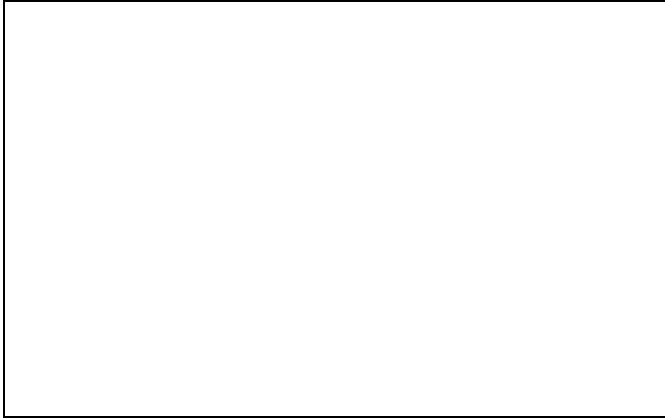


Fig. 9. Long-term evolution of the (logarithmic) deviation from sphericity at the half-mass radius for simulations with a softening length $\varepsilon = 0.01$ (solid, model F) and $\varepsilon = 0.02$ (dashed, model G) particles. The simulation was performed with $N = 16384$ particles.



Fig. 10. Long-term evolution of the (logarithmic) deviation from sphericity at the half-mass radius for simulations with a softening length $\varepsilon = 0.1$ (solid, model H) and $\varepsilon = 0.02$ (dashed, model G) particles. The simulations were performed with $N = 16384$ particles.

Figs. 6 and 11): first after the collapse the ROI leads to a triaxial configuration. In the second stage a fast readjustment of shape occurs during about 20 crossing times. Thereafter a steady relaxation follows until the system becomes axisymmetric ($b/a \approx 1$, but still $c/a \neq 1$) and finally spherical (Fig. 6). Later on the system does not change its shape (Fig. 7).

The timescale for spherization is given remarkably exact by the two-body relaxation time t_{rlx} of the N -body system. This is demonstrated in Fig. 7 by the temporal evolution of the minor-to-major axis ratio for two simulations with $N = 4096$ and $N = 16384$ and a softening length of $\varepsilon = 0.01$. The straight lines are no fits, but the slopes one gets by the assumption that spherization acts on a relaxation timescale. It should be noted that the good agreement can only be achieved when the Keplerian relaxation time is corrected for softening (for details see Theis (1998)). This gives a correction, i.e. an increase of the relaxation times, by approximately a factor of 3 for $N = 16384$.

The deviation from sphericity, $\delta(t) \equiv 1 - c/a(t)$, can be fitted by $\delta(t) \approx \delta(0) \exp(-t/t_{\text{rlx}})$ as the extended linear regime in Fig. 8 shows. Both, the dependence of the axis ratio evolution on the total number of particles (Fig. 8) and the softening length (Fig. 9 and 10) are in agreement with a spherization within a relaxation timescale of the softened two-body potential. The slow relaxation in model H ($\varepsilon = 0.1$) is due to the small ratio of maximum impact parameter to softening length (ε is twice the core radius!) which gives a strongly enhanced relaxation time.

Shortly after the initial collapse at t_{min} , however, the “relaxation” of shape of our models is much faster than one could expect from the two-body relaxation argument. This can be seen clearly in Fig. 11, which shows the long-term evolution of our reference model A1 ($N = 32768$, $\varepsilon = 0.01$). We denote this phase of fast shape change by the term “violent shape relaxation”. It is characterized by a substantially larger growth rate of the axis ratio as compared with expectations from two-body relaxation. Violent shape relaxation sets in after the ROI has established a triaxial configuration. Core radius and core mass do not vary strongly during violent shape relaxation (see Fig. 2a). Independent of taking 10% or 50% of the particles, the axis ratio growth rate during violent shape relaxation is constant for about 10–20 crossing times; thereafter a smaller growth rate obtained by two-body relaxation is following. Note that all variations of shape seen in Figs. 2–5 and discussed in subsection 2.2 are still in the violent phase and do not represent the long-term shape changes from two-body relaxation, which can be seen in the Figs. 6–11 for the long-term evolution.

3. Discussion and Summary

We performed a set of N -body simulations for the collapse of a dynamically cold Plummer sphere and studied the occurrence of radial orbit instability (ROI) and the evolution of shape. Especially, we focussed on the influence of the standard N -body parameters like the total number of particles or the softening length. Our simulations showed that the growth rate of the ROI is strongly changed by the softening at constant particle number and almost unaffected by a variation of N at constant softening. For our standard models with $\varepsilon = 0.01$ and $N = 16384$ ($N = 4096$), however, we could show by comparison with high-accuracy zero softening models, that no more artificial softening-dependent effects are present. But our results

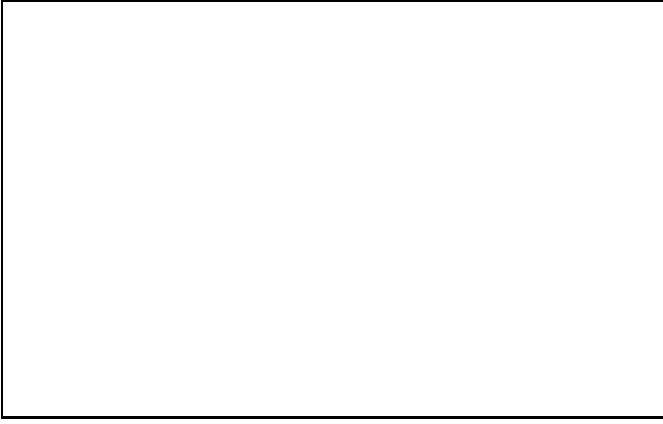


Fig. 11. Long-term evolution of the minor-to-major axis ratio in the centre (10% most bounded particles, dashed) and at the half-mass radius (solid) for model A1 ($N=32768$, $\varepsilon = 0.01$).

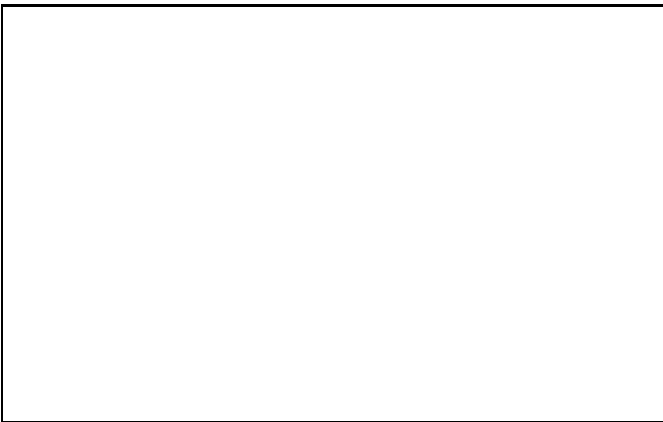


Fig. 12. Temporal evolution of the distance of the density centre from the centre of mass (solid) in correlation with Lagrangian radii (0.1%, 20%, 50%, dashed) for model A1 ($N=32768$, $\varepsilon = 0.01$).

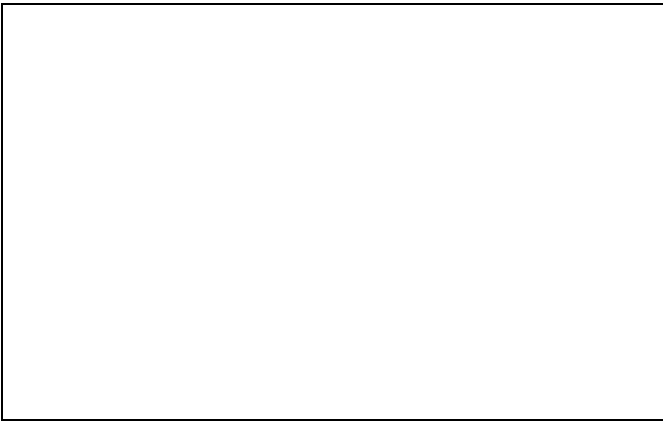


Fig. 13. Long-term evolution of the minor-to-major axis ratio at the half-mass radius for simulations with a softening length $\varepsilon = 0.01$ (solid, model A1) and $\varepsilon = 0.02$ (dashed, model C). The simulations were performed with $N = 32768$ particles.

show that for a given particle number inappropriate softening could yield wrong results by changing the collective effects as

well as the undesired two-body relaxation. Such findings are consistent with recent arguments given by Steinmetz & White (1997), Moore et al. (1997), and Fukushige & Makino (1997), in the context of N -body simulations for cosmological structure formation.

Generally, according to our simulations, the cold collapse with ROI and the subsequent evolution could be subdivided into three phases. First there is an initial strong collapse and build-up of triaxiality via ROI, characterized by a time t_{\min} at which a minimum value of the principal axis ratios c/a and b/a is obtained. Here our results agree with the findings of Hozumi, Fujiwara & Kan-ya (1996) insofar that the system remains spherical until maximum collapse $t_{\text{coll}} < t_{\min}$; it is only at that stage that strong anisotropies of the velocity dispersions create a triaxial configuration. This is also consistent with arguments by Bettwieser & Spurzem (1986) and Hensler et al. (1995), who state that homologously collapsing systems have to stay isotropic.

Second, a phase of rapid, violent shape relaxation occurs. It is much faster than by any estimate due to two-body relaxation. The mechanism of such violent shape relaxation is still unclear. We observe, however, strong fluctuations of the density centre of the system just during that phase, which are strongly correlated with oscillations of the Lagrangian radii of up to 20% of the total mass (see Fig. 12, here Lagrangian radii have not been measured with respect to the density centre but with respect to the centre of mass of the system). Even the half-mass radius varies due to these quasi-oscillations of the core whereas the 0.1% Lagrange radius is completely inside the core and, thus, not affected by the core's motion. We conclude that the rapid initial collapse induces strong motions of the density centre, which decay on a timescale of some ten crossing times. However, we saw that the core is already formed after two crossing times and does not change any more. This means, that a core fixed in size moves in the central region, by this inducing strong potential fluctuations which give rise to a relaxation which is added to the unavoidable two-body relaxation. When the core settles down these large-scale potential fluctuations disappear and the additional relaxation does not operate any more by this defining the last stage of shape evolution. A comparison of two long-term simulations with different softening lengths strengthens that point, insofar as it seems that two-body relaxation does not change the violent shape relaxation (Fig. 13): Whereas a difference in the relaxation rate in the last stage after $t = 20$ is obvious, the shape evolution is qualitatively almost unaffected during the violent shape relaxation stage. However, the relatively short timescale of violent shape relaxation and the scatter in the measured c/a -values makes a quantitative comparison impossible. It is interesting to compare with the similar problem of core oscillations in quasi-statically evolving spherical star cluster undergoing core collapse (Makino & Sugimoto 1987, Heggie, Inagaki & McMillan 1994, Spurzem & Aarseth 1996), which seem to occur on a similar timescale.

Finally, a third phase is observed, which is characterized by a secular drift of the system via axisymmetry towards spherical symmetry. It occurs on a time scale consistent with that of two-body relaxation, provided the proper softening is taken into account (Theis 1998).

Acknowledgements. This work was supported by the DFG grants Sp 345/5-1,2,3 and 446 JAP-113/18/0 (for travel). R.Sp.

and Ch.Th. wish to thank D. Sugimoto, J. Makino, M. Taiji, and all other colleagues from Dept. of Arts and Sciences, Komaba Campus, Univ. of Tokyo, for their continuous support in all GRAPE-related problems and their warm hospitality during our visits in Tokyo. Numerical computations were carried out on GRAPE 3Af (Kiel) and HARP-2 (Heidelberg) special purpose computers and partly at HLRZ Jülich. Last, but not least the authors want acknowledge the valuable comments of the referee, Roger Fux.

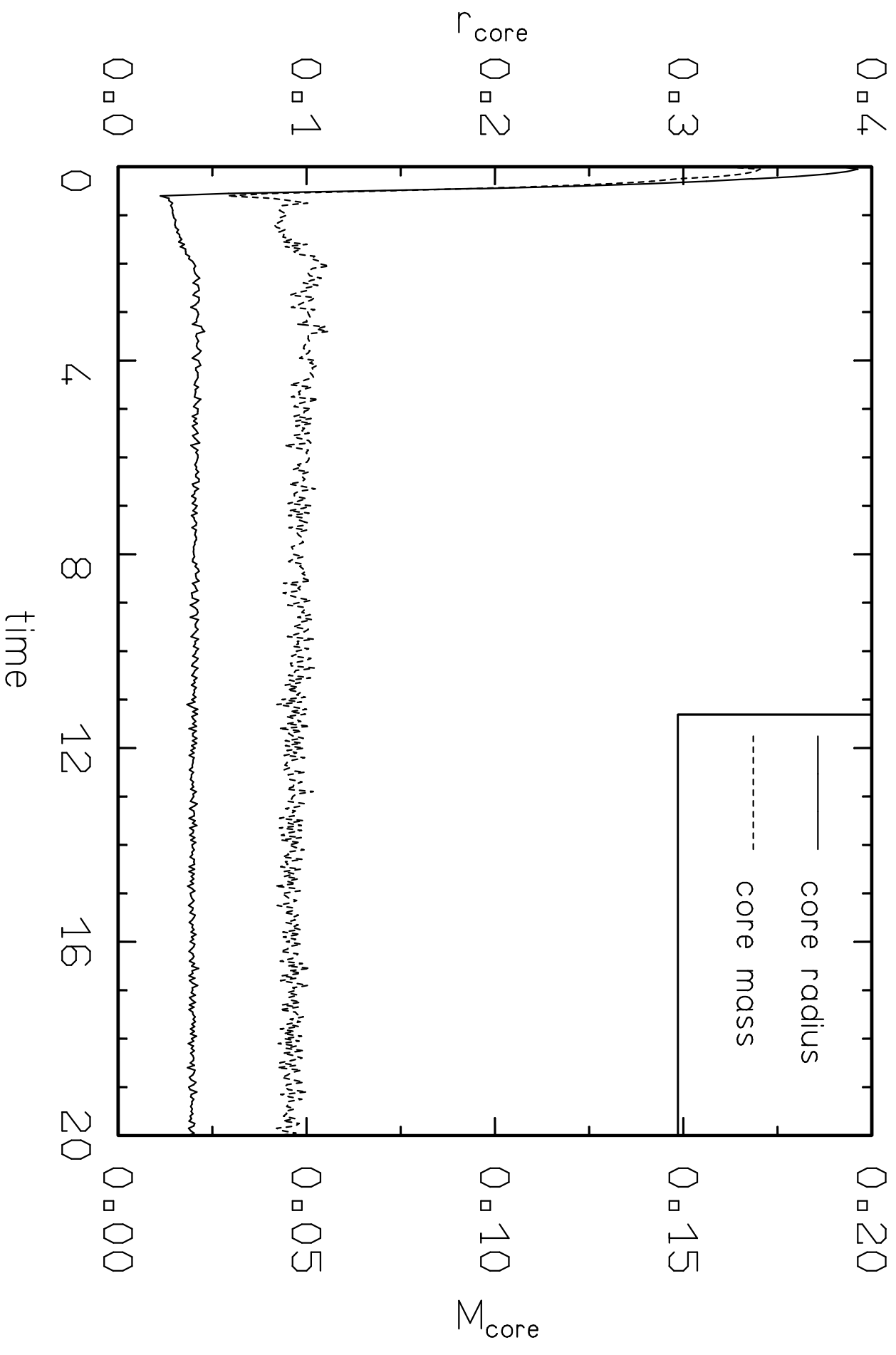
References

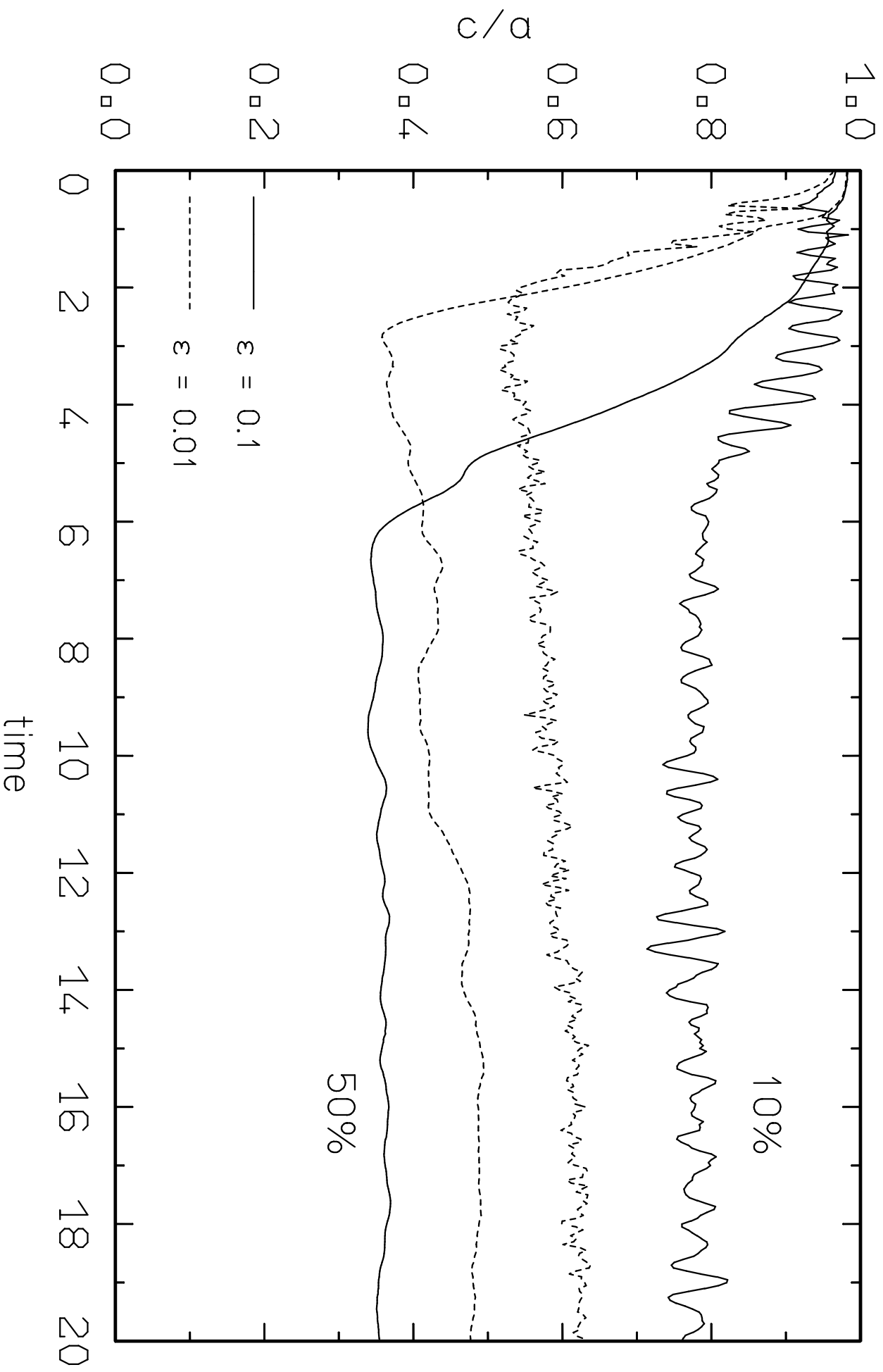
- Aguilar L.A., Merritt D.: 1990, *Astrophys. J.* **354**, 33
 van Albada, T.S.: 1982, *Monthly Notices Roy. Astron. Soc.* **201**, 939
 Antonov V.A.: 1961, *Soviet Astron.* **4**, 859
 Antonov V.A.: 1962, *Vest. Leningrad Gos. Univ.* **7**, 135.
 Barnes, J., Hut, P.: 1986, *Nature* **324**, 446
 Binney J., Tremaine, S.: *Galactic Dynamics*, Princeton Univ. Press (1987)
 Bettwieser E., Spurzem R.: 1986, *Astron. Astrophys.* **161**, 102
 Boily C.M., Clarke C.J., Murray S.D.: 1998, *Monthly Notices Roy. Astron. Soc.* , in press
 Burkert A.: 1990, *Monthly Notices Roy. Astron. Soc.* **247**, 152
 Cannizzo J.K., Hollister T.C.: 1992, *Astrophys. J.* **400**, 58
 Casertano S., Hut P.: 1985, *Astrophys. J.* **298**, 80
 Cuperman S., Goldstein S., Lecar M.: 1969, *Monthly Notices Roy. Astron. Soc.* **146**, 161
 Davé R., Dubinski J., Hernquist L.: 1997, *New Astronomy* **2**, 277
 Fukushige T., Makino J.: 1997, *Astrophys. J.* **477**, L9
 Heggie D.C., Inagaki S., McMillan S.L.W.: 1994, *Monthly Notices Roy. Astron. Soc.* **271**, 706
 Hensler G., Spurzem R., Burkert A., Trassl E.: 1995, *Astron. Astrophys.* **303**, 299
 Hernquist L., Ostriker J.P.: 1992, *Astrophys. J.* **386**, 375
 Hozumi S., Fujiwara T., Kan-ya Y.: 1996, *Publ. astr. Soc. Jap.* **48**, 503
 Hozumi S., Hernquist L.: 1995, *Astrophys. J.* **440**, 60
 Ipser J.R., Thorne K.S.: 1968, *Astrophys. J.* **154**, 251
 Kulsrud R.M., Mark J.W-K.: 1970, *Astrophys. J.* **160**, 471
 Lynden-Bell D.: 1964, in *IAU symp. No. 25*, p. 78.
 Lynden-Bell D.: 1967, *Monthly Notices Roy. Astron. Soc.* **136**, 101
 Makino J.: 1996, *Astrophys. J.* **471**, 796
 Makino J.: 1997, *Astrophys. J.* **478**, 58
 Makino J., Ebisuzaki T.: 1996, *Astrophys. J.* **465**, 527
 Makino J., Sugimoto D.: 1987, *Publ. astr. Soc. Jap.* **39**, 589
 Makino J., Taiji M., Ebisuzaki T., Sugimoto D.: 1997, *Astrophys. J.* **480**, 432
 Merritt D., Aguilar L.A.: 1985, *Monthly Notices Roy. Astron. Soc.* **217**, 787
 Min K.W., Choi C.S.: 1989, *Monthly Notices Roy. Astron. Soc.* **238**, 253
 Moore B., Governato F., Quinn T., Stadel J., Lake G. : 1997, *Astrophys. J.* , preprint astro-ph 9709051
 Polyachenko V.L., Shukhman I.G.: 1981, *Soviet Astron.* **25**, 533
 Spitzer L., Hart M.H.: 1971, *Astrophys. J.* **164**, 399
 Spurzem R.: 1998, *Monthly Notices Roy. Astron. Soc.* , subm.
 Spurzem R., Aarseth S.J.: 1996, *Monthly Notices Roy. Astron. Soc.* **282**, 19
 Steinmetz M., White S.D.M.: 1997, *Monthly Notices Roy. Astron. Soc.* **288**, 545
 Sugimoto D., Chikada Y., Makino J., Ito T., Ebisuzaki T., Umemura M.: 1990, *Nature* **345**, 33
 Theis Ch., Hensler G.: 1993, *Astron. Astrophys.* **280**, 85
 Theis Ch., Hensler G.: 1995, in *Galaxies in the Young Universe*, Hippelein H. (ed.), Ringberg, p. 201
 Theis Ch.: 1998, *Astron. Astrophys.* **330**, 1180
 Udry S.: 1993, *Astron. Astrophys.* **268**, 35
 Wiechen H., Ziegler H.J., Schindler K.: 1988, *Monthly Notices Roy. Astron. Soc.* **232**, 623
 Ziegler H.J., Wiechen H.: 1989, *Monthly Notices Roy. Astron. Soc.* **238**, 1261
 Ziegler H.J., Wiechen H.: 1990, *Astrophys. J.* **362**, 595

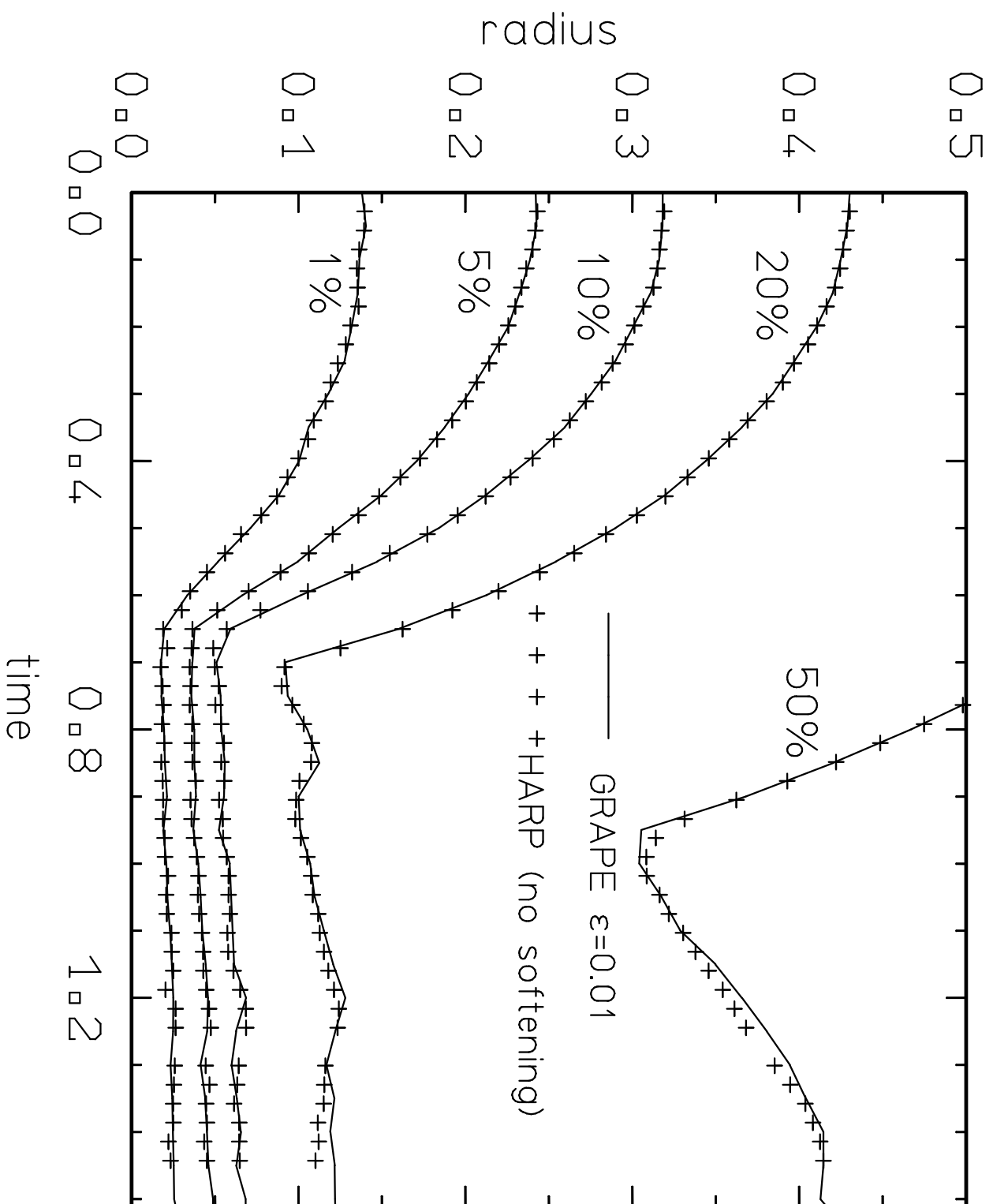
This article was processed by the author using Springer-Verlag \TeX A&A macro package 1991.

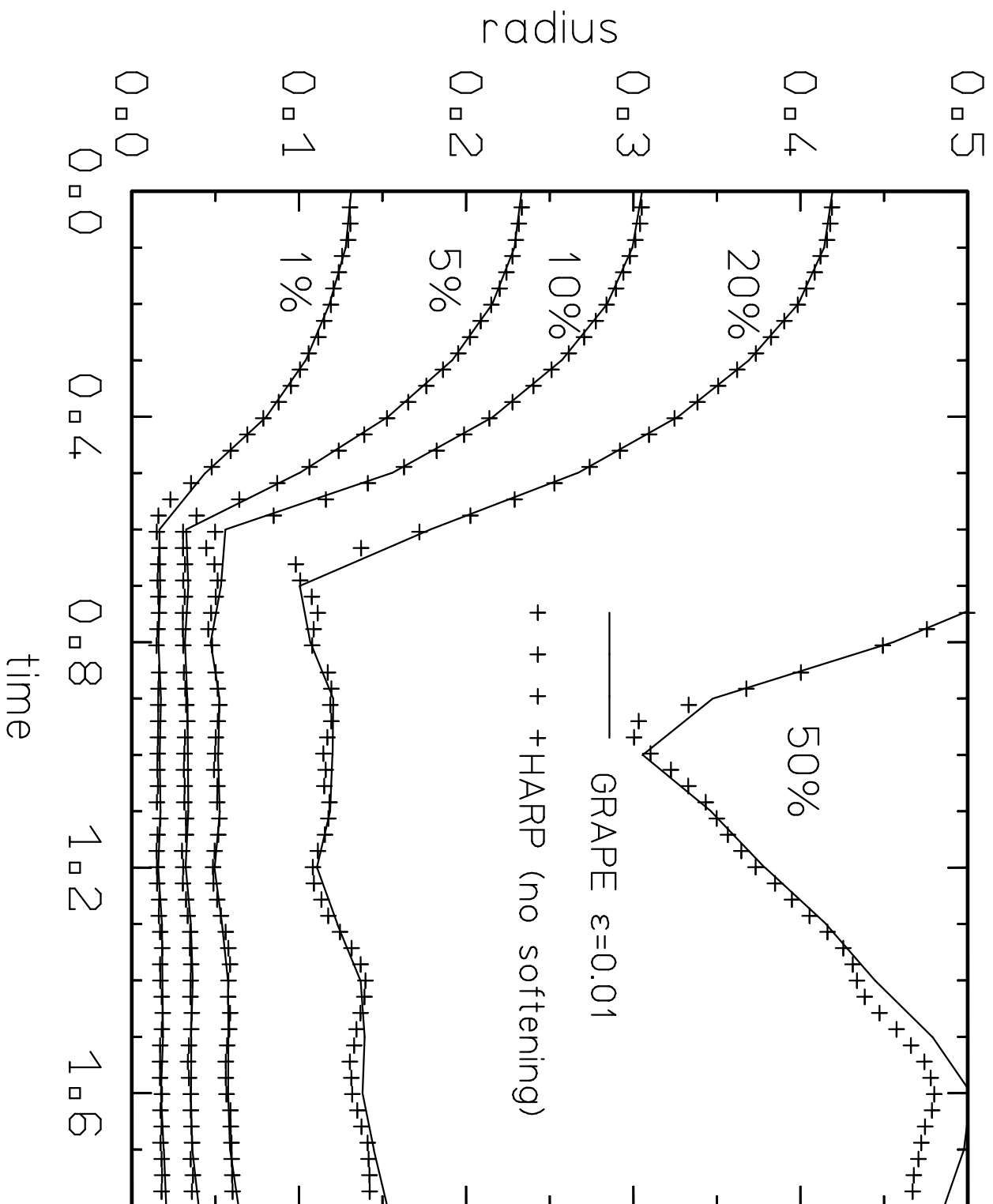
This figure "fig1.gif" is available in "gif" format from:

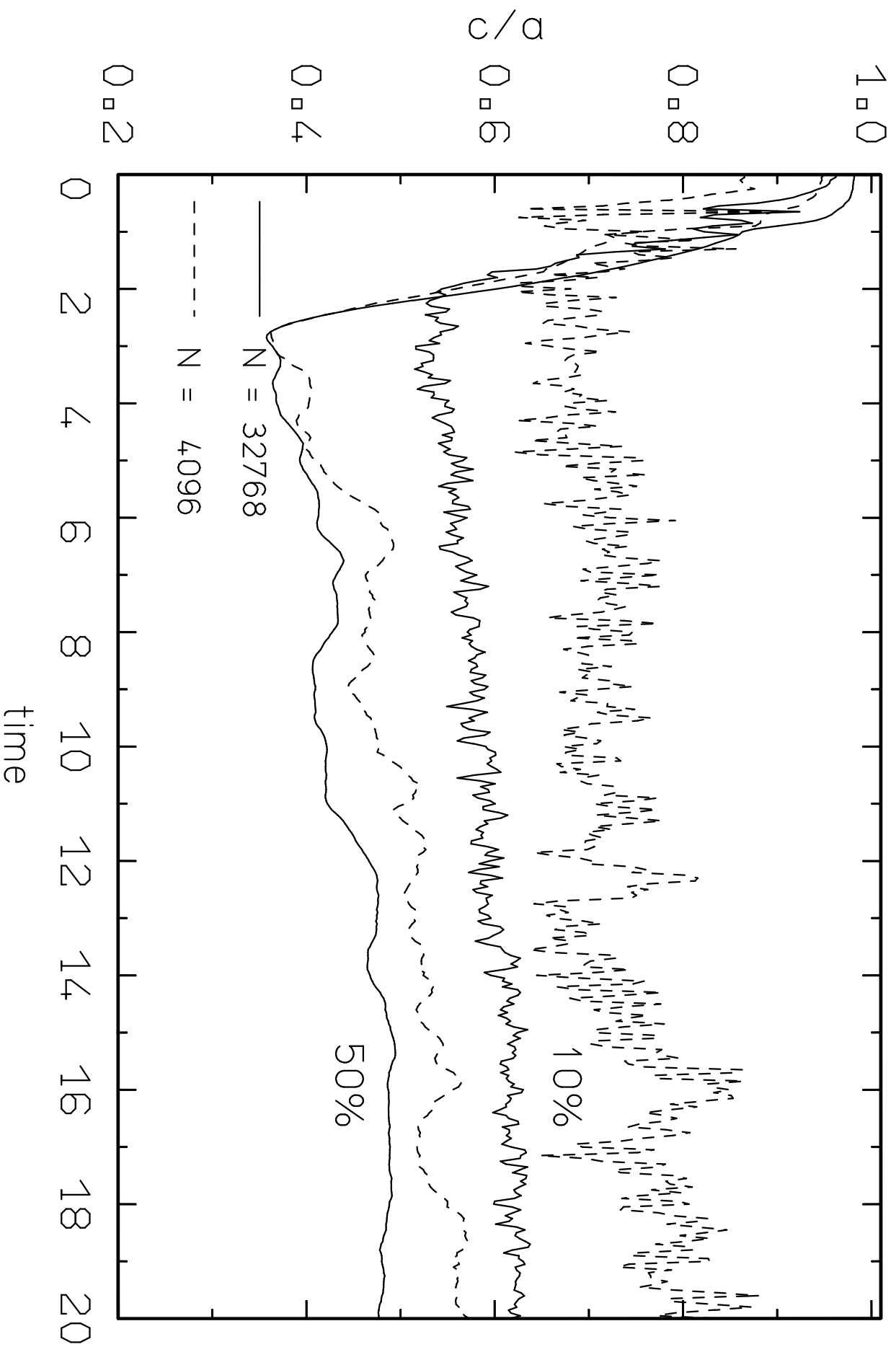
<http://arxiv.org/ps/astro-ph/9810023v1>

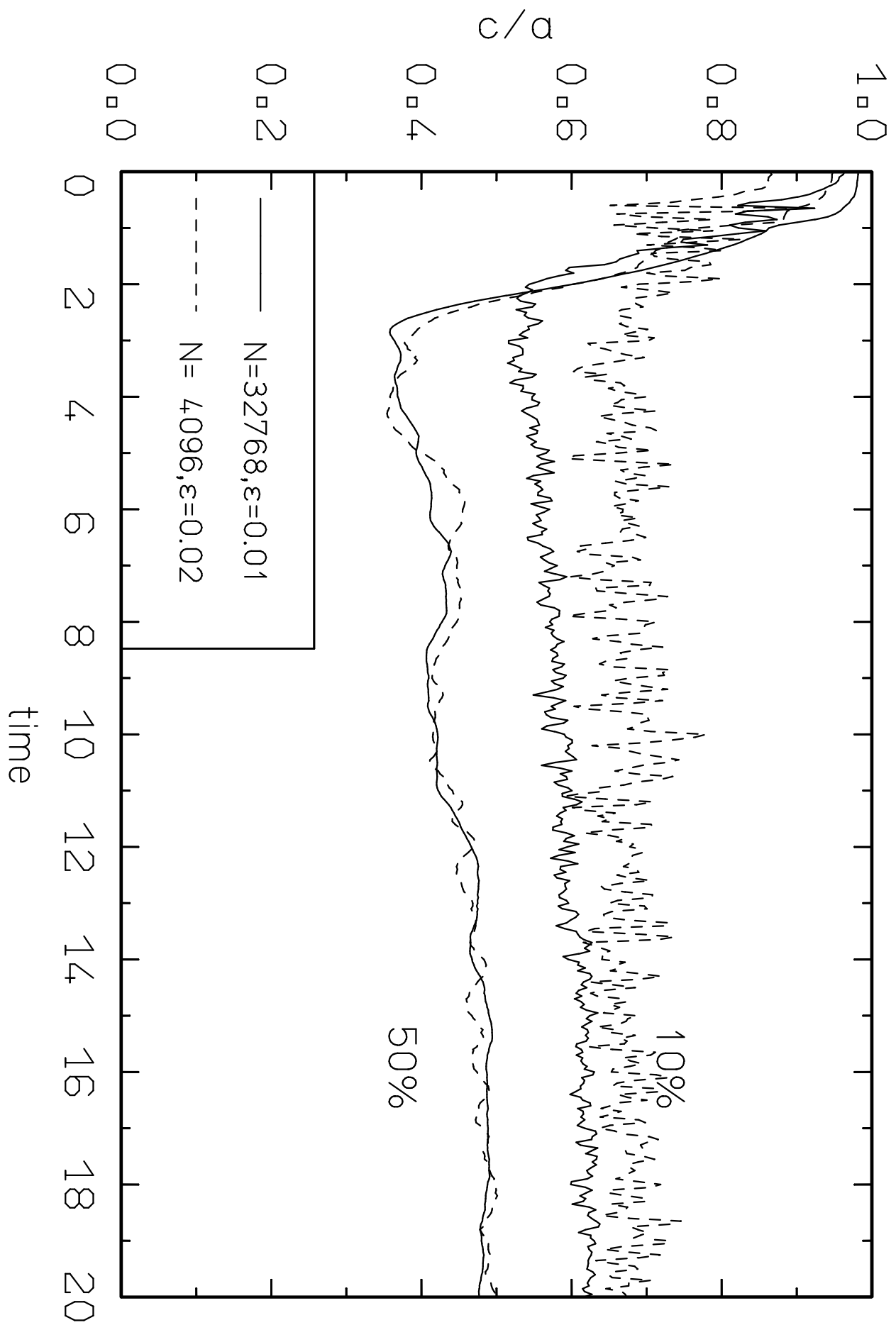


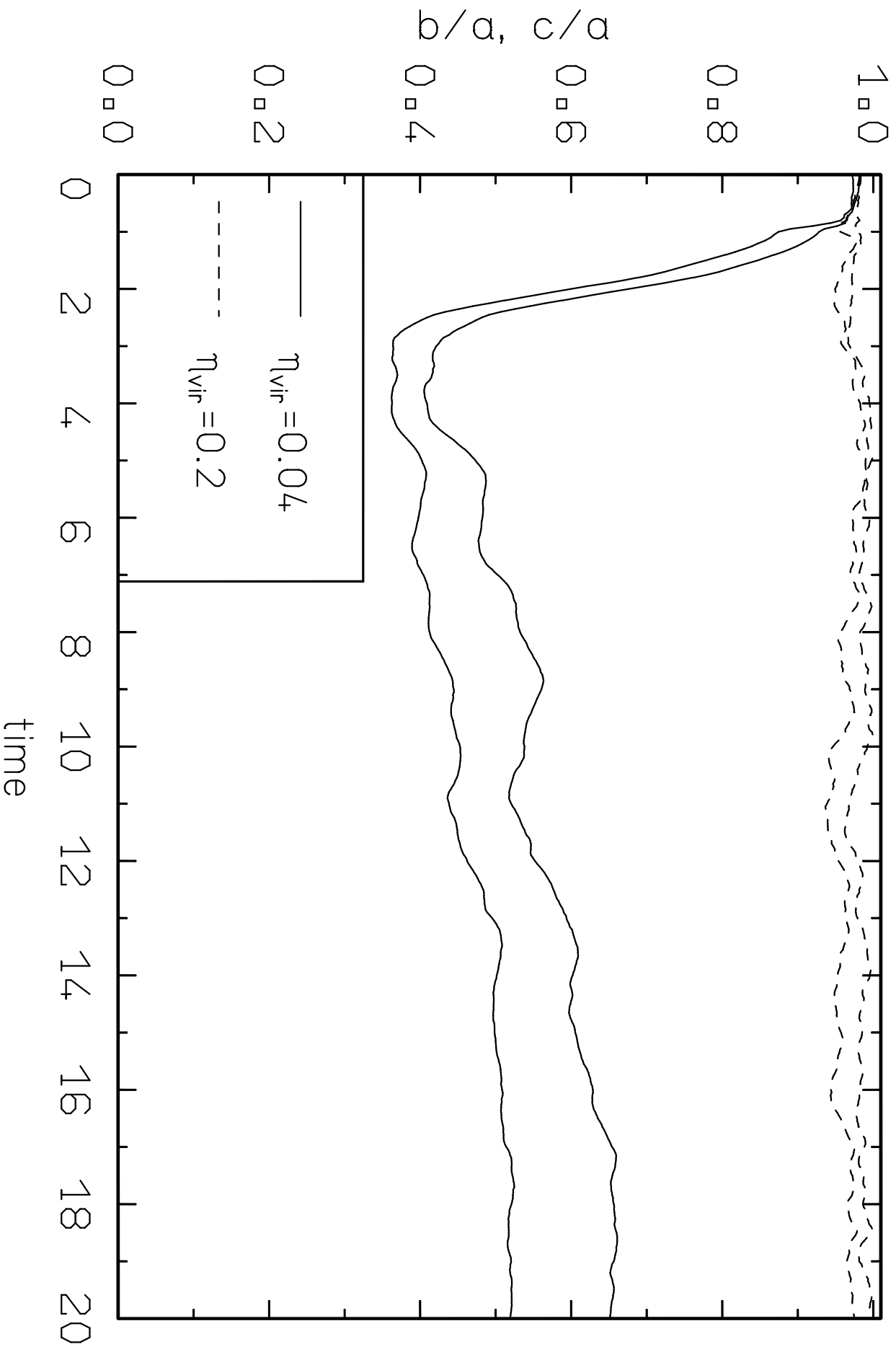






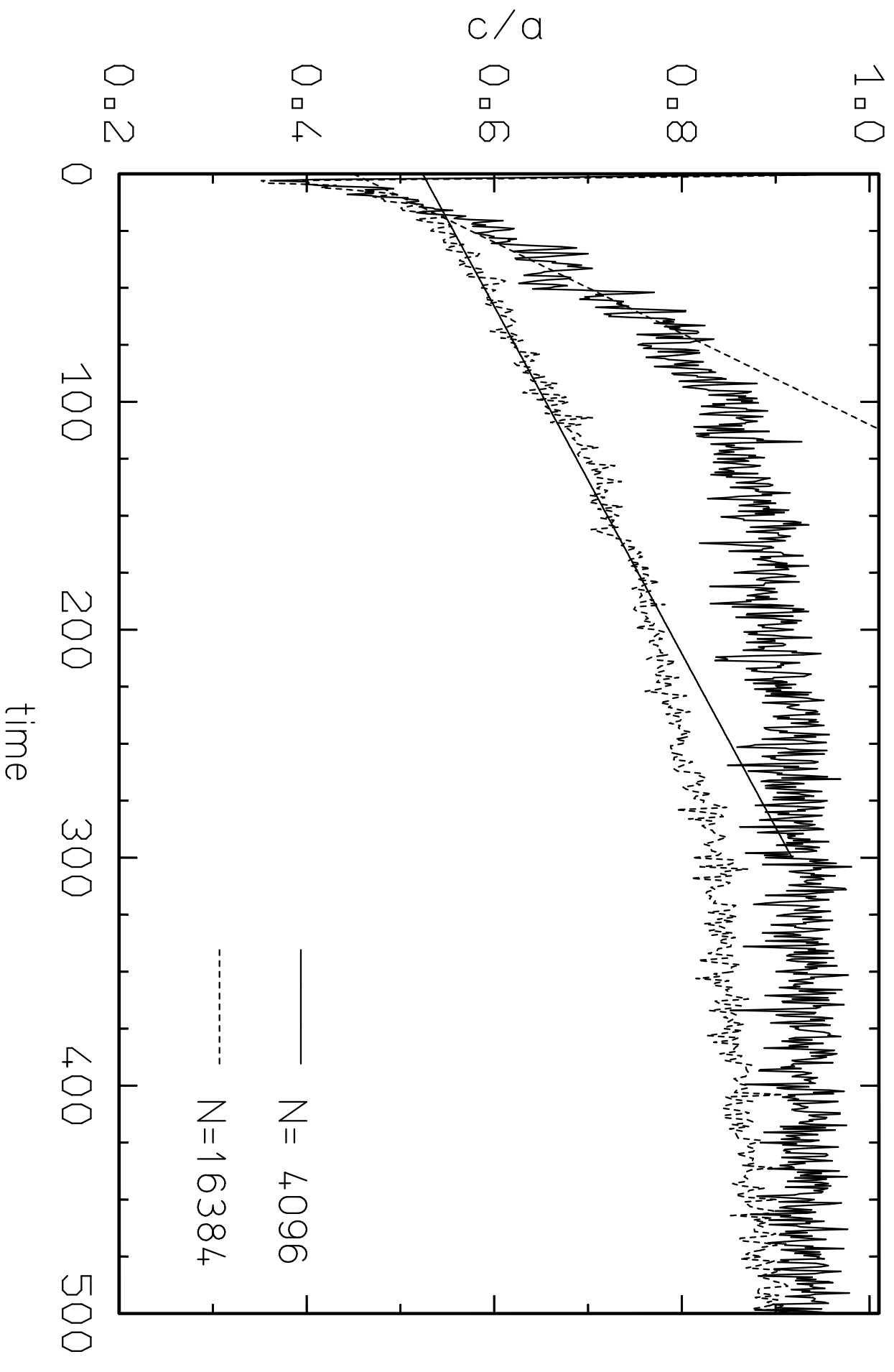






This figure "fig6.gif" is available in "gif" format from:

<http://arxiv.org/ps/astro-ph/9810023v1>



This figure "fig8.gif" is available in "gif" format from:

<http://arxiv.org/ps/astro-ph/9810023v1>

This figure "fig9.gif" is available in "gif" format from:

<http://arxiv.org/ps/astro-ph/9810023v1>

This figure "fig10.gif" is available in "gif" format from:

<http://arxiv.org/ps/astro-ph/9810023v1>

This figure "fig11.gif" is available in "gif" format from:

<http://arxiv.org/ps/astro-ph/9810023v1>

This figure "fig12.gif" is available in "gif" format from:

<http://arxiv.org/ps/astro-ph/9810023v1>

This figure "fig13.gif" is available in "gif" format from:

<http://arxiv.org/ps/astro-ph/9810023v1>